JOURNAL OF NATURAL PRODUCTS

Note

pubs.acs.org/jnp

Trichostatin Analogues JBIR-109, JBIR-110, and JBIR-111 from the Marine Sponge-Derived *Streptomyces* sp. RM72

Takahiro Hosoya,[†] Takatsugu Hirokawa,[‡] Motoki Takagi,*[,†] and Kazuo Shin-ya*[,§]

[†]Biomedicinal Information Research Center (BIRC), Japan Biological Informatics Consortium (JBIC), 2-4-7 Aomi, Koto-ku, Tokyo 135-0064, Japan

[‡]Computational Biology Research Center (CBRC), National Institute of Advanced Industrial Science and Technology (AIST), 2-4-7 Aomi, Koto-ku, Tokyo 135-0064, Japan

[§]Biomedicinal Information Research Center (BIRC), National Institute of Advanced Industrial Science and Technology (AIST), 2-4-7 Aomi, Koto-ku, Tokyo 135-0064, Japan

Supporting Information

ABSTRACT: Three new trichostatin analogues, JBIR-109 (**1**), JBIR-110 (**2**), and JBIR-111 (**3**), were isolated from the culture of the marine sponge-derived *Streptomyces* sp. strain RM72, together with trichostatin A (**4**) and trichostatic acid (**5**). The planar structures of **1**−**3** were determined on the basis of extensive NMR and MS analyses. In addition, the absolute configurations of the amino acid residues were determined by Marfey's method. The histone deacetylase inhibitory activities of **1**−**5** were examined, and their structure−activity relationships are discussed.

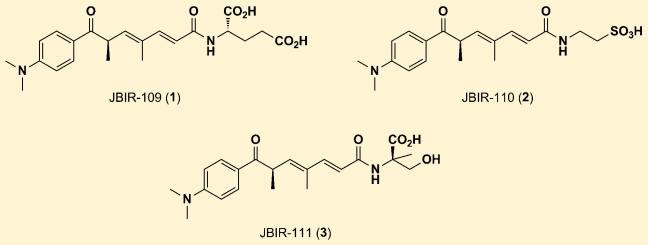

Histone deacetylases (HDACs) play an important role in the epigenetic regulation of gene expression by catalyzing the deacetylation of lysine residues in histone proteins, stimulating chromatin condensation, and promoting transcriptional repression.[1,2] Human HDACs are divided into five classes/subclasses on the basis of their homology to yeast HDACs: class I (HDAC1, 2, 3, and 8), class IIa (HDAC4, 5, 7, and 9), class IIb (HDAC6 and 10), class III (SIRT1, 2, 3, 4, 5, 6, and 7), and class IV (HDAC11). Because aberrant epigenetic changes are hallmarks of cancer, HDACs are promising targets for the development of anticancer drugs. Inhibitors of HDACs can induce cell-cycle arrest, differentiation, and tumor cell death. In fact, several HDAC inhibitors are currently in clinical trials for the treatment of both solid and hematologic malignancies.[1,2]

In our search for HDAC inhibitors, we isolated a novel trichostatin analogue, JBIR-17, in which a serine residue is attached to C-1 of trichostatic acid via an amide bond, from the culture of *Streptomyces* sp. 26634.[3] Upon further screening, we discovered three additional trichostatin analogues, JBIR-109 (**1**), JBIR-110 (**2**), and JBIR-111 (**3**), from the culture of *Streptomyces* sp. RM72, which was associated with a marine sponge collected from a mesopelagic area. We report herein the isolation, structure elucidation, and biological activities of **1**−**3**.

Streptomyces sp. RM72 was cultured in production medium with 50% artificial seawater. Compounds **1**−**3**, together with trichostatin A (**4**)[4] and trichostatic acid (**5**),[5] were recovered from the culture supernatant by using HP-20 resin, followed by purification with sequential chromatography utilizing MPLC and HPLC.

The structures of **1**−**3** were primarily elucidated by spectroscopic analyses. The presence of an amide functional group was suggested by an IR absorption at 1650 cm^{-1}. The UV absorption maxima at 340 and 264 nm, together with ^{1}H and ^{13}C NMR data for **1**−**3** (Table 1 and Table S1), suggested that the basic structural skeletons were identical to that of **5**. Detailed structural information was obtained from the HSQC, HMBC, and DQF-COSY spectra of **1**−**3** (Figure 1).

The molecular formula of **1** was established as $C_{22}H_{28}N_2O_6$ on the basis of HRESIMS data ($[M + H]^+$; *m/z*, 417.2029). In addition to the trichostatic acid portion of the structure, the sequence from the α-methine proton H-2′ (δ_H 4.50; δ_C 53.5) to methylene protons H-4′ (δ_H 2.40) through methylene protons H-3′ (δ_H 1.98, 2.20) was observed. HMBC correlations between H-3′ and two carboxylic carbonyl carbons, C-1′ (δ_C 175.3) and C-5′ (δ_C 176.5), suggested a glutamic acid moiety. Finally, HMBC correlations between both the olefinic proton H-2 and the α-methine proton H-2′ and an amide carbonyl carbon C-1 (δ_C 169.0) established the structure of **1** as a glutamate-substituted trichostatic acid.

The molecular formulas of **2** and **3** were determined to be $C_{19}H_{26}N_2O_5S$ and $C_{21}H_{28}N_2O_5$ on the basis of the HRESIMS data ($[M + H]^+$, *m/z* 395.1655 and $[M + H]^+$, *m/z* 389.2067), respectively. The trichostatic acid core structure in **2** and **3** was established on the basis of NMR data similarly to that described for **1**. For **2**, a COSY correlation between the amino methylene protons H-1′ (δ_H 3.67, δ_C 36.7) and methylene protons H-2′

Received: October 17, 2011
Published: January 25, 2012

Chart 1

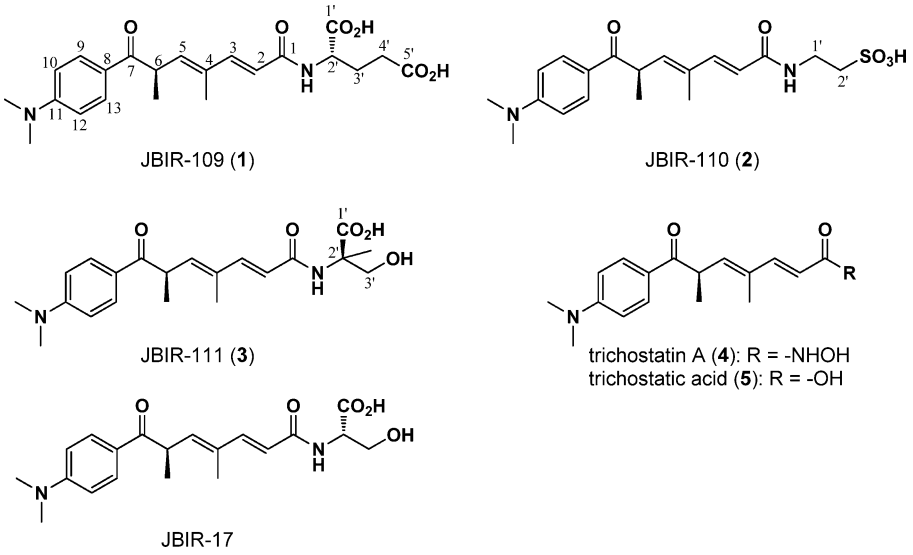

Table 1. ^{1}H (600 MHz) and ^{13}C (150 MHz) NMR Spectroscopic Data for JBIR-109 (1) in CD_3OD

position	δ_C, type	δ_H (J in Hz)
1	169.0, C	
2	120.3, CH	6.09, d (15.5)
3	146.6, CH	7.16, d (15.5)
4	134.5, C	
5	141.5, CH	5.91, d (9.5)
6	41.8, CH	4.53, dq (6.5, 9.5)
7	201.5, C	
8	124.8, C	
9, 13	132.0, CH	7.86, d (9.0)
10, 12	112.0, CH	6.73, d (9.0)
11	155.5, C	
4-methyl	12.8, CH_3	1.95, s
6-methyl	18.3, CH_3	1.27, d (6.5)
11-*N*,*N*-dimethyl	40.1, CH_3	3.06, s
Glu		
1′	175.3, C	
2′	53.5, CH	4.50, dd (6.0, 9.0)
3′	28.3, CH_2	2.20, m
		1.98, m
4′	31.4, CH_2	2.40, m
5′	176.5, C	

(δ_H 2.99), together with an HMBC correlation from H-1′ to amide carbonyl carbon C-1 (δ_C 168.7), revealed that an additional two-carbon fragment was present at the carboxy terminus of the trichostatic acid skeleton. The NMR spectra of the amino acid moiety [C-1′ (δ_H 3.67, δ_C 36.7) and C-2′ (δ_H 2.99, δ_C 51.4)] in **2** were similar to those of taurine [C-1′ (δ_H 3.55, δ_C 36.8) and C-2′ (δ_H 2.95, δ_C 51.5)] in the literature.[6] Finally, a sulfonic acid residue, the presence of which was deduced from the molecular formula, was attached to H-2′, establishing that **2** was a trichostatic acid analogue modified with taurine as shown in Figure 1.

The NMR spectroscopic data for **3** closely resembled those of JBIR-17. An HMBC correlation from the singlet methyl protons 3′-Me (δ_H 1.48) to carboxy carbonyl carbon C-1′ (δ_C 177.1), quaternary carbon C-2′ (δ_C 62.4), and a hydroxymethyl carbon (δ_C 66.0) suggested the presence of an α-methylserine moiety. The molecular formula of **3** indicated a C-2′-methylated congener of JBIR-17. In addition, the connectivity of trichostatic acid and the α-methylserine moiety was confirmed by NMR experiments in DMSO-d_6. HMBC correlations between the amide proton (δ_H 7.85) and C-1 (δ_C 164.6), C-1′ (δ_C 174.8), C-2′ (δ_C 60.0), C-3′ (δ_C 65.2), and 1′-methyl (δ_C 20.1) indicated that the α-methylserine connects to C-1 of trichostatic acid through an amide bond.

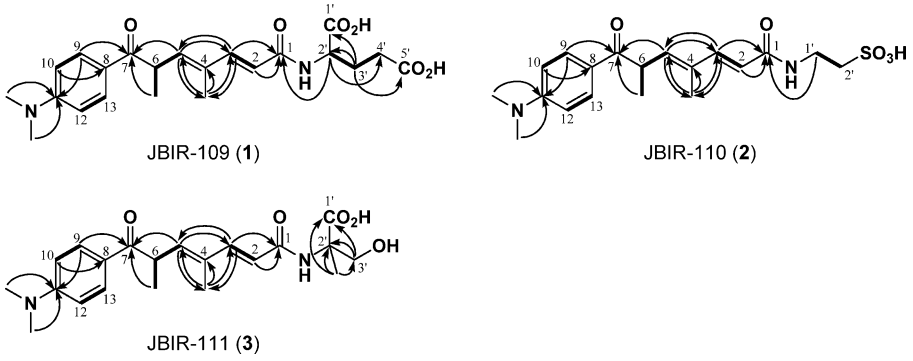

Figure 1. Key correlations observed in 2D NMR spectra of **1**, **2**, and **3**. Bold lines show ^{1}H–^{1}H DQF-COSY correlations, and arrows show HMBC results.

dx.doi.org/10.1021/np200843k | *J. Nat. Prod.* 2012, 75, 285–289

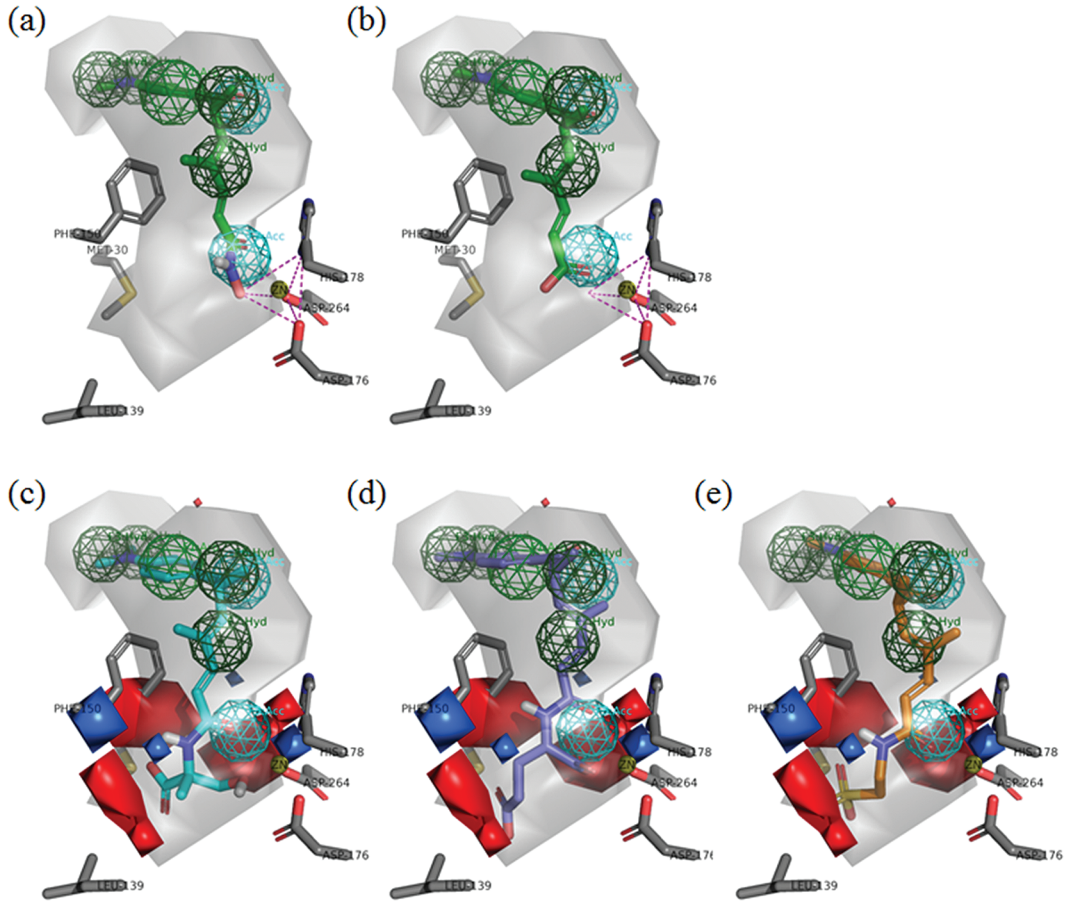

Figure 2. Proposed binding models for **4** (a), **5** (b), **1** (c), **2** (d), and **3** (e) to human HDAC1. Carbon atoms of **1** (purple, blue), **2** (orange), and **3** (cyan) are shown. Consensus features of the pharmacophore models are generated for the five molecules: hydrogen bond acceptor (cyan feature), aromatic ring region (green feature), and hydrophobic region (dark green feature). The shape of the overall volume for the five molecules is defined by the transparent surface. HDAC1 residues around the compounds are shown in stick (gray) representation. Tetrahedral zinc complexes in the protein cavity, which are composed of a nitrogen atom of a histidine residue, two carbonyl groups of aspartic acid residues, and the carbonyl group of the compounds, are represented by the polyhedral cage with purple dashed lines in (a) and (b). Red and blue in (c, d, e) show negative and positive regions, respectively, predicted by electrostatic analysis using 3D-QSAR.

The absolute configurations of the glutamic acid residue in **1** and the α-methylserine residue in **3** were defined by Marfey's method.[7] Comparisons of retention times between the FDAA-treated residues from the hydrolysates of standards established the configurations of the glutamic acid residue in **1** as L and the α-methylserine residue in **3** as *R*. It is intriguing to note that the configuration of the serine in **3** is opposite that of the serine in JBIR-17 isolated from another *Streptomyces* sp.[3] Because the specific rotation value ($[\alpha]^{25}_{D}$ +29, *c* 0.10, MeOH) of **4** isolated with **1**−**3** is of the same sign and similar to the value ($[\alpha]^{25}_{D}$ +63 (*c* 0.10, MeOH)[4]) reported for **4**, the absolute configurations of the trichostatic acid residues of **1**−**3** are proposed to be the same as for (*R*)-trichostatin A.[4]

To evaluate the HDAC inhibitory activity of **1**−**5**, we employed HDAC1 as a representative HDAC. The IC_{50} values against HDAC1 of **1**−**5** were 48, 74, 57, 0.012, and 73 μM, respectively. The inhibitory activities of **1**−**3** and **5** against HDAC1 were >1000 times weaker than that of **4**. These results are consistent with the reported model for HDAC1 inhibition by trichostatin A, in which the hydroxamate functionality is essential to exert the activity.[8] In addition, we performed computational binding analyses using the 3D-quantitative structure−activity relationship (QSAR) for **1**−**5** (Figure 2). The results show that the main reason for the low binding affinity of **5** to HDAC1 can be ascribed to the inability to form a stable tetrahedral zinc complex in the protein cavity. Meanwhile, the electrostatic analysis by 3D-QSAR showed that the low-binding affinity of **1**−**3** is due to an unfavorable interaction between the hydrophobic surface consisting of Leu-139, Phe-150, and Met-30 within the protein cavity and the polar functional groups in these compounds.

HDAC inhibitors are promising antitumor agents and also play important roles as low-molecular probes to study epigenetics. These results provide valuable information for developing new HDAC inhibitors.

EXPERIMENTAL SECTION

General Experimental Procedures. Optical rotations were measured using a Horiba SEPA-300 polarimeter. UV and IR spectra were measured with a Beckman Coulter DU730 UV/vis spectrophotometer and a Horiba FT-720 spectrophotometer, respectively. NMR spectra were collected in CD_3OD using a Varian NMR System 600 NB CL spectrometer with the residual solvent peaks referenced to δ_C 49.15 and δ_H 3.31 ppm. The optimizations of HMBC and HSQC spectra for appropriate couplings were 8 and 140 Hz, respectively. HRESIMS data were recorded using a Waters LCT-Premier XE mass spectrometer. Reversed-phase MPLC was conducted on a Purif-Pack ODS-100 column (Shoko Scientific). Analytical reversed-phase HPLC was conducted using an XBridge C18 column (4.6 i.d. × 150 mm;

dx.doi.org/10.1021/np200843k | *J. Nat. Prod.* 2012, 75, 285−289

Waters) in conjunction with a Waters 2996 photodiode array detector and a Waters 3100 mass detector. Analytical reversed-phase UPLC (Waters) was performed using a BEH ODS column (2.1 i.d. × 50 mm; Waters) in conjunction with a Waters ACQUITY UPLC photodiode array eλ detector and an LCT-Premier XE mass spectrometer. Preparative reversed-phase HPLC was conducted using an XBridge Prep C18 column (20 i.d. × 150 mm) in conjunction with a Hitachi High Technologies L-2455 photodiode array detector.

Biological Material. *Streptomyces* strain RM72 was isolated from an unidentified marine sponge collected at a depth of 195 m at the position 28° 53′ 35.8″ N, 129° 29′ 57.0″ E near Takara Island, Kagoshima Prefecture, Japan. To identify the strain, a partial 16S rRNA gene sequence was determined (DDBJ accession number AB683042), and comparison with sequences in the Eztaxon type strain database[9] revealed that the closest phylogenetic neighbor of the strain was *Streptomyces angustmycinicus* NBRC 3934^T (AB184817), with a sequence identity of 100%.

Fermentation. The strain was cultivated in 50 mL test tubes each containing 15 mL of the seed medium consisting of 1.0% starch (Kosokagaku), 1.0% Polypepton (Nihon Pharmaceutical), 1.0% molasses (Dai-Nippon Meiji Sugar), and 1.0% meat extract (Extract Ehlrich, Wako Pure Chemical Industry) (pH 7.2). The test tubes were shaken on a reciprocal shaker (320 rpm) at 27 °C for 2 days. Aliquots (2.5 mL) of the broth were then transferred to 500 mL baffled Erlenmeyer flasks containing 100 mL of the production medium consisting of 1.0% starch, 1.0% glucose (Kanto Chemical), 1.0% glycerin (Nacalai Tesque), 0.5% Polypepton, 0.2% yeast extract (BD Biosciences), 1.0% corn-steep liquor (Oriental Yeast), 0.1% NaCl (Kanto Chemical), and 0.32% $CaCO_3$ (Kozaki Pharmaceutical) in 50% artificial seawater (Marine art SF-1, Tomita Pharmaceutical) (pH 7.4 before sterilization) and cultured on a rotary shaker (180 rpm) at 27 °C for 5 days.

Isolation. The fermentation broth (2 L) was separated into the mycelial cake and supernatant by centrifugation. The supernatant was subsequently applied to a Diaion HP-20 column, and the column was then washed with H_2O and eluted with 100% MeOH. After evaporation of the 100% MeOH eluent *in vacuo*, the resulting residue was subjected to reversed-phase MPLC by using an aqueous MeOH linear gradient system (20−100% MeOH). The 20−30% MeOH eluate (145 mg) was then subjected to preparative reversed-phase HPLC with 55% aqueous MeOH containing 0.1% formic acid (flow rate, 6 mL/min) to give JBIR-109 (**1**, t_R = 13.7 min, 3.5 mg) and JBIR-110 (**2**, t_R = 11.3 min, 3.4 mg). In addition, the 30−40% MeOH eluate (107 mg) was purified by preparative reversed-phase HPLC using 58% aqueous MeOH containing 0.1% formic acid (flow rate, 6 mL/min) to give JBIR-111 (**3**, t_R = 13.7 min, 3.5 mg), trichostatin A (**4**, t_R = 11.3 min, 0.7 mg), and trichostatic acid (**5**, t_R = 13.0 min, 1.0 mg).

JBIR-109 (1): colorless, amorphous solid; $[\alpha]^{25}_D$ −27 (*c* 0.10, MeOH); UV (MeOH) λ_{max} (log ε) 340 (4.2), 265 (4.2) nm; IR (KBr) ν_{max} 1660 cm^{-1}; ^{1}H NMR (600 MHz, CD_3OD) and ^{13}C NMR (150 MHz, CD_3OD), see Table 1; HRESIMS *m*/*z* 417.2029 $[M + H]^+$ (calcd for $C_{22}H_{29}N_2O_6$, 417.2026).

JBIR-110 (2): colorless, amorphous solid; $[\alpha]^{25}_D$ +12 (*c* 0.10, MeOH); UV (MeOH) λ_{max} (log ε) 340 (4.2), 264 (4.2) nm; IR (KBr) ν_{max} 1660 cm^{-1}; ^{1}H NMR (600 MHz, CD_3OD) and ^{13}C NMR (150 MHz, CD_3OD), see Table 2; HRESIMS *m*/*z* 395.1655 $[M + H]^+$ (calcd for $C_{19}H_{27}N_2O_5S$, 395.1641).

JBIR-111 (3): colorless, amorphous solid; $[\alpha]^{25}_D$ +33 (*c* 0.10, MeOH); UV (MeOH) λ_{max} (log ε) 340 (4.1), 265 (4.2) nm; IR (KBr) ν_{max} 1650 cm^{-1}; ^{1}H NMR (600 MHz, CD_3OD) and ^{13}C NMR (150 MHz, CD_3OD), see Table 2; HRESIMS *m*/*z* 389.2067 $[M + H]^+$ (calcd for $C_{21}H_{29}N_2O_5$, 389.2076).

Determination of Amino Acid Configurations. A sample of **1** or **3** (1.0 mg) was hydrolyzed in 6 N HCl (0.2 mL) at 110 °C for 12 h. After acid hydrolysis, the reaction solution was adjusted to neutral pH and evaporated *in vacuo*. The residue was dissolved in 10 mL of EtOAc−H_2O (1:1). The amino acid mixture was then recovered in the aqueous layer. After drying the aqueous layer *in vacuo*, it was dissolved in 5% $NaHCO_3$ (600 μL), and FDAA (Marfey's reagent, 0.2 mg) in acetone (600 μL) was added. The mixture was then heated in an oil bath at 70 °C for 10 min with frequent shaking. The reaction products were analyzed by the UPLC system. A Waters BEH ODS column was developed with 20% aqueous MeCN containing 0.1% formic acid at a flow rate of 0.3 mL/min. The retention times of the FDAA derivatives were determined by monitoring UV absorption at 340 nm and the positive mode of ESIMS. The retention times of the standard FDAA derivatives were as follows: L-Glu, 2.34 min; D-Glu, 2.95 min; α-methyl-*R*-Ser, 2.10 min; and α-methyl-*S*-Ser, 2.74 min. The retention times of the FDAA derivatives from **1** and **3** were 2.38 min for Glu and 2.10 for α-methyl-Ser, respectively.

Table 2. ^{1}H (600 MHz) and ^{13}C (150 MHz) NMR Spectroscopic Data for Amino Acid Moieties of JBIR-110 (2) and JBIR-111 (3) in CD_3OD

JBIR-110 (**2**)			JBIR-111 (**3**)		
position	δ_C, type	δ_H (*J* in Hz)	position	δ_C, type	δ_H (*J* in Hz)
Taurine			MeSer		
1′	36.7, CH_2	3.67, t (6.6)	1′	177.1, C	
2′	51.4, CH_2	2.99, t (6.6)	2′	62.4, C	
			3′	66.0, CH_2	3.90, brd (11.0)
					3.85, brd (11.0)
			3′-methyl	20.8, CH_3	1.48, s

HDAC1 Inhibitory Assay. The human HDAC1 inhibitory activity was evaluated using the HDAC1 inhibitor screening assay kit (Cayman Chemical) according to the manufacturer's protocol. Briefly, 140 μL of assay buffer, 10 μL of diluted HDAC1, and 10 μL of samples were added in a 96-well black plate. To initiate the reaction, 10 μL of the HDAC substrate (final concentration, 200 μM) was added. After incubation for 30 min at 37 °C, 40 μL of the developer was added and mixed. After further incubation for 15 min at room temperature, the fluorescence (excitation, 340 nm; emission, 450 nm) was measured. Trichostatin A was used as a positive control (IC_{50} = 12 nM).

Quantitative Structure−Activity Relationship. 3D-QSAR analysis for compounds **1**−**5** was carried out using the homology model of HDAC1 and the docking simulation. A three-dimensional structure of human HDAC1 was constructed by a homology modeling approach with the structural template of the crystal structure of an HDAC homologue complexed with trichostatin A (PDB-ID: 1C3R),[10] incorporated in the program Prime with default parameters (Schrödinger, LLC). The sequence identity between HDAC1 and the HDAC homologue protein was 32% (see Supporting Information, Figure 24S). The structural template was selected by using a similarity measure from the sequence-structure alignment and in addition from the protein−ligand interactions in the active-site environment obtained by induced fit modeling. To prepare the compounds with active conformations for 3D-QSAR analysis, molecular models of the compound-bound HDAC1 were generated by docking simulation using Glide SP mode with default parameters (Schrödinger, LLC). The grid center for docking was defined using the reference position of trichostatin A on 1C3R, which is the structural template used in the homology modeling step. 3D-QSAR analysis with the aligned active conformation from docking results was performed using the Auto-GPA protocol on MOE (Chemical Computing Group). The visualizations were generated by PyMOL (Schrödinger, LLC).

■ ASSOCIATED CONTENT

Ⓢ Supporting Information

^{1}H and ^{13}C NMR, DQF-COSY, HSQC, CT-HMBC, and HRESIMS spectra of **1**−**3** are available free of charge via the Internet at http://pubs.acs.org.

AUTHOR INFORMATION

Corresponding Author

*(M.T.) Tel: +81-3-3599-8305. Fax: +81-3-3599-8494. E-mail: motoki-takagi@aist.go.jp. (K.S.) Tel: +81-3-3599-8305. Fax: +81-3-3599-8494. E-mail: k-shinya@aist.go.jp.

ACKNOWLEDGMENTS

This work was supported by a grant from the New Energy and Industrial Technology Department Organization (NEDO). The sponge was collected during the NT-09-17 cruise of Natsushima, by the Japan Agency for Marine-Earth Science and Technology (JAMSTEC).

REFERENCES

(1) Carew, J. S.; Giles, F. J.; Nawrocki, S. T. *Cancer Lett.* **2008**, *269*, 7−17.
(2) Shankar, S.; Srivastava, R. K. *Adv. Exp. Med. Biol.* **2008**, *615*, 261−298.
(3) Ueda, J.; Hwang, J. H.; Maeda, S.; Kato, T.; Ochiai, A.; Isshiki, K.; Yoshida, M.; Takagi, M.; Shin-ya, K. *J. Antibiot.* **2009**, *62*, 283−285.
(4) Morikawa, H.; Ishihara, M.; Takezawa, M.; Hirayama, K.; Suzuki, E.; Komoda, Y.; Shibai, H. *Agric. Biol. Chem.* **1985**, *49*, 1365−1370.
(5) Tsuji, N.; Kobayashi, M.; Nagashima, K.; Wakisaka, Y.; Koizumi, K. *J. Antibiot.* **1976**, *29*, 1−6.
(6) Bi, D.; Chai, X.-Y.; Song, Y.-L.; Lei, Y.; Tu, P.-F. *Chem. Pharm. Bull.* **2009**, *57*, 528−531.
(7) Marfey, P. *Carlsberg Res. Commun.* **1984**, *49*, 591−596.
(8) Yoshida, M.; Kijima, M.; Akita, M.; Beppu, T. *J. Biol. Chem.* **1990**, *265*, 17174−17179.
(9) Chun, J.; Lee, J. H.; Jung, Y.; Kim, M.; Kim, S.; Kim, B. K.; Lim, Y. W. *Int. J. Syst. Evol. Microbiol.* **2007**, *57*, 2259−2261.
(10) Finnin, M. S.; Donigian, J. R.; Cohen, A.; Richon, V. M.; Rifkind, R. A.; Marks, P. A.; Breslow, R.; Pavletich, N. P. *Nature* **1999**, *401*, 188−193.